communications earth & environment

ARTICLE

https://doi.org/10.1038/s43247-023-01065-0 OPEN

# A 37-year record of ocean acidification in the Southern California current

Wiley H. Wolfe [1], Todd R. Martz [1✉], Andrew G. Dickson[1], Ralf Goericke[1] & Mark D. Ohman[1]

Long-term ocean time series have proven to be the most robust approach for direct observation of climate change processes such as Ocean Acidification. The California Cooperative Oceanic Fisheries Investigations (CalCOFI) program has collected quarterly samples for seawater inorganic carbon since 1983. The longest time series is at CalCOFI line 90 station 90 from 1984–present, with a gap from 2002 to 2008. Here we present the first analysis of this 37- year time series, the oldest in the Pacific. Station 90.90 exhibits an unambiguous acidification signal in agreement with the global surface ocean (decrease in pH of $-0.0015 \pm 0.0001\,yr^{-1}$), with a distinct seasonal cycle driven by temperature and total dissolved inorganic carbon. This provides direct evidence that the unique carbon chemistry signature (compared to other long standing time series) results in a reduced uptake rate of carbon dioxide ($CO_2$) due to proximity to a mid-latitude eastern boundary current upwelling zone. Comparison to an independent empirical model estimate and climatology at the same location reveals regional differences not captured in the existing models.

[1] Scripps Institution of Oceanography, University of California San Diego, La Jolla, CA, USA. ✉email: trmartz@ucsd.edu

Atmospheric carbon dioxide ($CO_2$) levels today are nearly 50% higher than during pre-industrial times and are predicted to increase at similar or accelerating rates over the next hundred years[1]. The ocean has taken up roughly a quarter of the total anthropogenic emissions[2], resulting in decreased ocean pH and associated changes in carbonate system equilibrium due to ocean acidification (OA)[3]. Globally, the mean surface ocean pH has decreased by ~0.1 since the beginning of the Industrial Revolution and is projected to drop by as much over the next 60 years[4,5]. These trends have been modeled[6] and detected[7] in the California Current System (CCS).

The California Cooperative Oceanic Fisheries Investigation (CalCOFI) program was formed in 1949 to study the pelagic ecosystem of the CCS in response to the collapse of an economically important sardine fishery[8]. The original sampling design included regular cruises making a grid pattern of profiles to 500 m of physically and biologically important parameters such as temperature, salinity, and zooplankton biomass. Observations of carbonate chemistry were incorporated into CalCOFI in 1983 at the same time as Charles David Keeling initiated time series measurements at Hydrostation S near Bermuda[9], and Olafsson and Takahashi began a time series in the North Atlantic[9–11]. The most continuous time series in the Southern CCS is surface waters (0–20 m) at CalCOFI Line 90 Station 90 (station 90.90). Observations were made at this location between 1984–present, with a gap from 2002 to 2008. Station 90.90 is the oldest traditional hydrographic time series of inorganic carbon in the Pacific yet, these valuable observations have remained unpublished until this work. The long-term trends established by this work add a direct observation of OA and climate change to the few existing time series of ocean carbonate chemistry[9,12].

CalCOFI station 90.90 is located at 31.4°N, 122°W, approximately 450 km from shore, with a water depth of approximately 4000 m. Due to its location in the western California Current, station 90.90 lies near the eastern edge of the North Pacific Subtropical Gyre exhibiting an oligotrophic open-ocean regime[13] (the mean phosphate and nitrate concentrations were 0.3 µM and 0.1 µM respectively in sea surface samples with inorganic carbon observations). Samples were analyzed for total alkalinity ($A_T$) and dissolved inorganic carbon ($C_T$). $A_T$ and $C_T$ were used to calculate other carbonate system variables such as, partial pressure of $CO_2$ in seawater ($pCO_2$), pH, carbonate ion concentration ($[CO_3^{2-}]$), saturation states of aragonite and calcite ($\Omega_{aragonite}$, $\Omega_{calcite}$), and Revelle Factor ($\partial \ln[CO_2]/\partial \ln C_T$). See Methods for details.

## Results and discussion

The time series exhibits an unambiguous OA signal in pH of $-0.0015 \pm 0.0001$ yr$^{-1}$ from 1984 to 2021, in agreement with the global surface ocean average[14] of $-0.0017$ yr$^{-1}$ (Fig. 1, Table 1), as well as a distinct seasonal cycle (Fig. 1, right column). The sea surface $pCO_2$ at station 90.90 is driven by increasing total inorganic carbon ($C_T$) at a decadal scale and a combination of $C_T$ and temperature at a seasonal scale (Fig. 2). There is no significant trend in ocean temperature, salinity, $A_T$ or n$A_T$ at station 90.90. However, longer-term, near-shore studies in the CCE have shown increasing temperatures shoreward of the California Current[15].

Several features make station 90.90 unique compared to other multi-annual longstanding oceanic inorganic carbon time series[9]. Station 90.90 is the oldest traditional hydrographic inorganic carbon time series location in the Pacific, it is also the furthest from land globally. The observed $C_T$, $\Omega_{aragonite}$, Revelle Factor, sea surface temperature and salinity at station 90.90 have average seasonal ranges not covered by the other seven time series[9]. Station 90.90 is one of two located within an eastern boundary current, shown in Supplementary Fig. 1 (alongside European Station for Time series in the Ocean at the Canary Islands i.e., ESTOC)[9]. Station 90.90 is also one of two time series locations that appear to be annual net sources of $CO_2$ to the atmosphere (alongside CArbon Retention In A Colored Ocean i.e., CARIACO)[9,16]. Station 90.90 has a mid-range Revelle Factor, and a mean $pCO_2$ close to that of the atmosphere (Fig. 3), resulting in a nominal to low mean $\Delta pCO_2$, where $\Delta pCO_2$ is the difference in the partial pressure of $CO_2$ between the sea surface and atmosphere. All of the other time series sites are located in areas with either a lower Revelle Factor or a greater $\Delta pCO_2$. A lower Revelle Factor allows for greater uptake and storage of anthropogenic $CO_2$ and a greater (negative) $\Delta pCO_2$ increases the uptake of both natural and anthropogenic $CO_2$. The unique chemical signature of station 90.90 results in the lowest $CO_2$ uptake rate among all of the timeseries sites[9]. The direct evidence of a reduced uptake rate of $CO_2$, relative to the global average is presumably due to proximity to a mid-latitude eastern boundary current upwelling zone[17]. As we discuss below, this finding is significant because models prescribing climate change trends in terms of mean $C_T$ uptake rate will differ from those using local Revelle Factor and $\Delta pCO_2$.

Natural variability at station 90.90 (resulting from, e.g., interannual variability in the proportion of North Pacific Gyre vs California Current water masses) along with the six-year gap in data confound the identification of long period patterns such as El Nino, or the Pacific Decadal Oscillation. Perhaps the most obvious anomaly is a perturbation in temperature and salinity during 2014–2016 (Fig. 1). This anomaly may be a result of the 2014/15 North Pacific marine heatwave, the strong 2015/16 El Nino, or a combination of the two[18–20].

Power spectral density (PSD) analysis of the detrended time series showed the presence of a strong annual signal in temperature and $C_T$, as well as in all calculated carbonate system variables, but did not resolve interannual features within the time series (Supplementary Fig. 5). While temporal anomalies in this time series may be worthy of further investigation, the goal of this work is to present the 1st order OA trend, mean seasonal cycle, and to finally make the quality-controlled time series publicly available. Follow-on work with this time series may consider implementing gap-filling techniques for the 2002–2008 period[21] and alternative modes of trend detection such as simultaneous fitting of harmonics and underlying trends as well as development of a mixed layer carbon budget at station 90.90.

The station 90.90 observations presented here are compared to the global bottle dataset (Global Ocean Data Analysis Project; GLODAP[22]) and the global underway $pCO_2$ dataset (Surface Ocean $CO_2$ Atlas (SOCAT)[23]). GLODAP data are used via the widely-accepted open-source empirical function, ESPER[24]. SOCAT data are the basis of a product used in this study[25,26] to estimate the sea surface $pCO_2$ at station 90.90.

Using ESPER we estimate $C_T$ and $A_T$, where $C_T$ and $A_T$ are derived from local data collected independent of CalCOFI (see methods)[24]. While ESPER can also serve as the basis to estimate $pCO_2$, (as well as pH and Ω) products based on SOCAT provide a more robust comparison for $pCO_2$ due to the higher density of surface data in their training set. This was done using two different sets of predictor variables: first, using only temperature and salinity, and second, using all available predictor variables including temperature, salinity, phosphate, nitrate, silicic acid, and oxygen concentrations (in addition to latitude, longitude, depth, and year in both cases). Depending on the "preformed" nature of surface water, additional variables such as oxygen and nutrients may not correlate with carbonate parameters in the surface ocean, hence the use of T and S only as one set of predictors[27,28]. Using only temperature and salinity, the comparison for $C_T$ showed measurements were $6 \pm 15$ µmol kg$^{-1}$

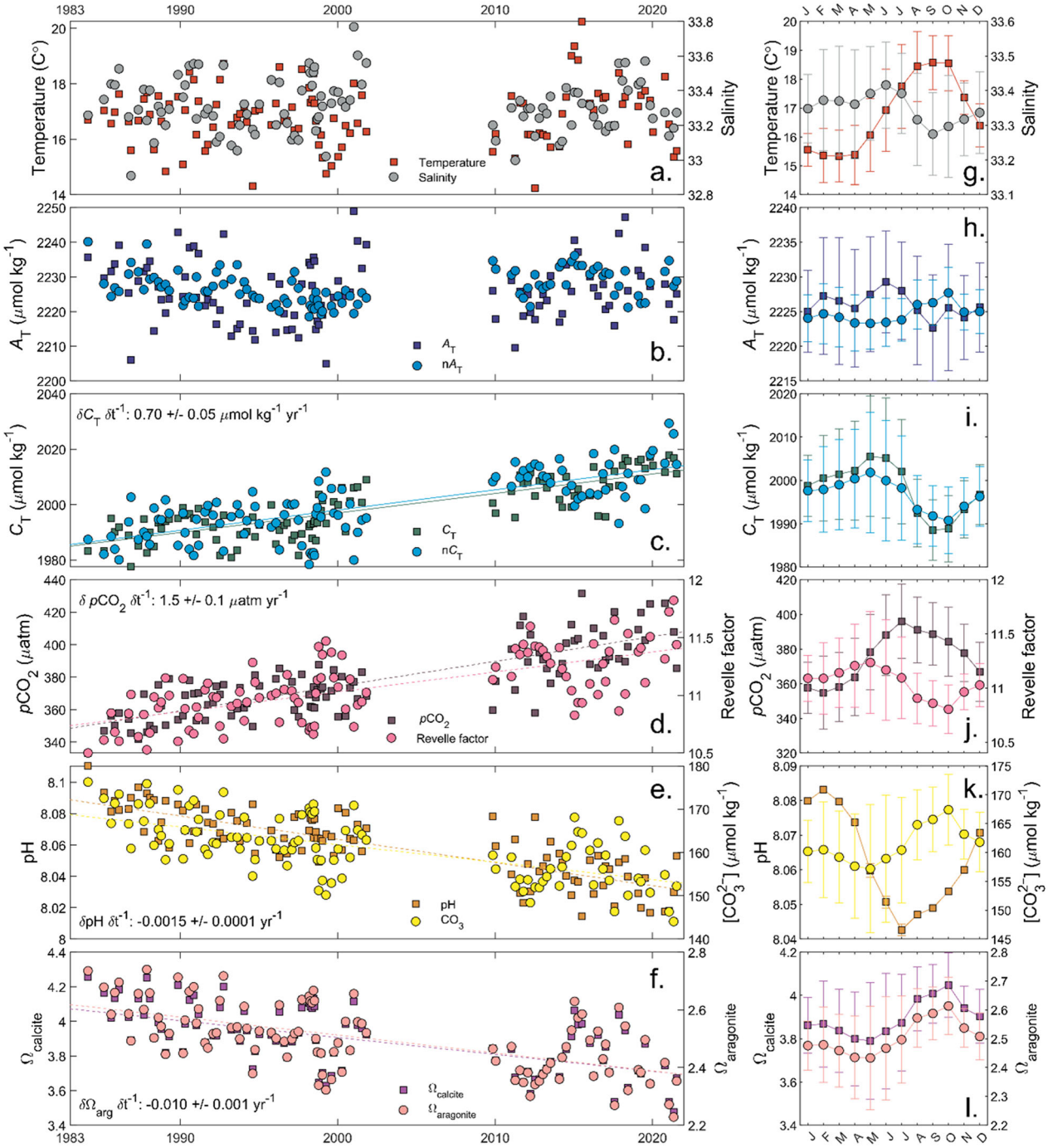


**Fig. 1 CalCOFI Line 90, Station 90 ocean time series.** Seasonally detrended observations (**a**–**f**) and average seasonal cycles (**g**–**l**). "n" indicates salinity normalization to the mean salinity (33.3). **a** Temperature and salinity, (**b**) Total alkalinity ($A_T$) and $nA_T$, (**c**) Total inorganic carbon ($C_T$) and $nC_T$, (**d**) $pCO_2$ (μatm) and Revelle factor, (**e**) pH and $CO_3$, and (**f**) $\Omega_{calcite}$ and $\Omega_{aragonite}$. There is no significant trend in temperature, salinity or $A_T$ ($p > 0.35$). The ocean acidification trend (shown in **c**–**f**) is within the range of observations made at other time series sites[9]. Regression statistics for time series are shown in Table 1. Descriptive statistics for seasonal cycles are shown in Supplementary Table 2. Error bars in (**g**–**l**) represent the standard error of the 3 month sliding bin (Supplementary Fig. 2) with number of observations ranging from 20 to 33.

(mean ± std) higher than ESPER with less variability (Supplementary Fig. 6). The comparison of $A_T$ showed measurements were 4 ± 4 μmol kg$^{-1}$ (mean ± std) lower than ESPER with similar variability (Supplementary Fig. 7). Both $C_T$ and $A_T$ are significantly different than the ESPER predictions ($p$«0.05). When using all available predictor variables, the comparison for $C_T$ showed measurements were 0.1 ± 6 μmol kg$^{-1}$ (mean ± std) higher than ESPER with similar variability (Supplementary Fig. 8). The comparison of $A_T$ showed measurements were 3 ± 4 μmol kg$^{-1}$ (mean ± std) different than ESPER with similar variability (Supplementary Fig. 9). Only $A_T$ was significantly different than the ESPER predictions ($p$«0.05). Increased accuracy in predicted $C_T$ and $A_T$ when using a greater number of predictor variables matches ESPER's expected performance[24].

There was no significant trend in the $A_T$ residuals when using either set of predictor variables. However, there was a significant

**Table 1 Regression statistics of sea surface hydrography and seawater carbon chemistry from 1984 to 2021. (from Fig. 1).**

| Parameter | Slope | standard error | units | *n* | $r^2$ | *p*-value |
|---|---|---|---|---|---|---|
| Hydrography | | | | | | |
| Temperature | 0.0078 | 0.009 | °C $yr^{-1}$ | 107 | 0.0070 | 0.3927 |
| Salinity | −0.0005 | 0.0013 | $yr^{-1}$ | 107 | 0.0012 | 0.7273 |
| Ocean acidification indicators | | | | | | |
| pH | −0.0015 | 0.0001 | $yr^{-1}$ | 105 | 0.6711 | <0.0001 |
| $CO_3^{2-}$ | −0.41 | 0.05 | µmol $kg^{-1}$ $yr^{-1}$ | 105 | 0.4064 | <0.0001 |
| $\Omega_{calcite}$ | −0.0097 | 0.0012 | $yr^{-1}$ | 105 | 0.4022 | <0.0001 |
| $\Omega_{aragonite}$ | −0.0062 | 0.0008 | $yr^{-1}$ | 105 | 0.3698 | <0.0001 |
| Seawater carbonate chemistry | | | | | | |
| $C_T$ | 0.70 | 0.05 | µmol $kg^{-1}$ $yr^{-1}$ | 107 | 0.6624 | <0.0001 |
| $nC_T$ | 0.73 | 0.06 | µmol $kg^{-1}$ $yr^{-1}$ | 107 | 0.5573 | <0.0001 |
| $A_T$ | 0.03 | 0.08 | µmol $kg^{-1}$ $yr^{-1}$ | 105 | 0.0012 | 0.7288 |
| $nA_T$ | 0.06 | 0.04 | µmol $kg^{-1}$ $yr^{-1}$ | 105 | 0.0246 | 0.1103 |
| $pCO_2$ | 1.53 | 0.11 | µatm $yr^{-1}$ | 105 | 0.6681 | <0.0001 |
| Revelle factor | 0.017 | 0.002 | $yr^{-1}$ | 105 | 0.4652 | <0.0001 |

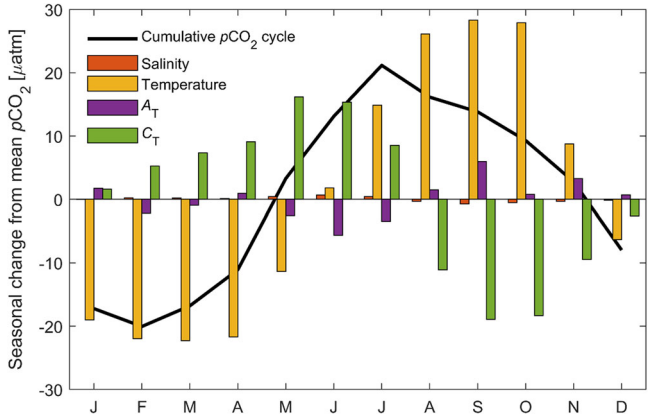


**Fig. 2 Forcings on the annual $pCO_2$ cycle.** The relative contributions of salinity, temperature, $A_T$ and $C_T$ to the seasonal cycle of sea surface $pCO_2$, computed using CO2SYS[40].

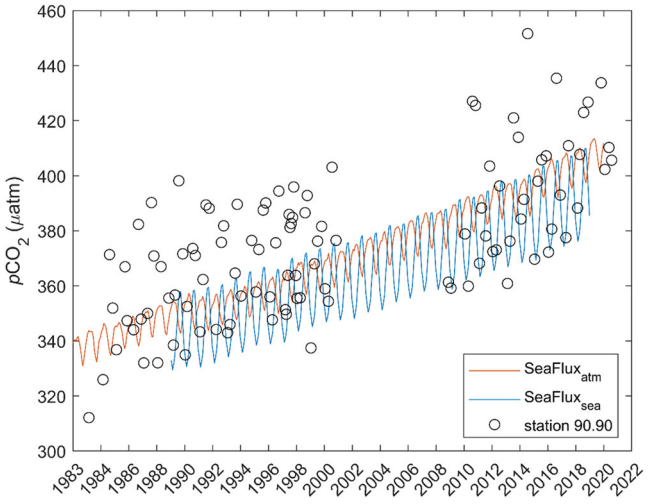


**Fig. 3 Comparison of $pCO_2$.** Data products[26] for atmospheric boundary layer ($SeaFlux_{atm}$) and sea surface $pCO_2$ ($SeaFlux_{sea}$) compared to sea surface $pCO_2$ at station 90.90. SeaFlux data are the average between two points, longitude 121.5°W, 31.5°N and 122.5°W, 31.5°N. From Table 2 in ref. [25], the reported bias ± RMSE (relative to the training data) in the product used to generate $SeaFlux_{sea}$ is 0.1 ± 13.7 µatm.

trend in the $C_T$ residuals in both sets of predictor variables (Supplementary Figs. 6 and 8), indicating the predicted $C_T$ trend was 40% higher (a residual slope of 0.3 higher than the measured slope of 0.7 µmol $kg^{-1}$ $yr^{-1}$) than the observed trend. Both sets of predictor variables resulted in the same trend, albeit with a higher standard deviation when using fewer predictors. The discrepancy between the OA trend observed and predicted may be due to the use of the simplified steady-state assumption used by ESPER to predict anthropogenic $CO_2$ as a function of time via a simple exponential equation with one coefficient applied globally[24]. We noted a slight decrease in phosphate over the time series (Wolfe, 2022), which could impact the trend in the second ESPER prediction, but not the first. The decrease in phosphate may signal a change in biogeochemistry of the region and is worth further investigation, but the fact a discrepancy of 0.3 µmol $kg^{-1}$ $yr^{-1}$ shows up in both versions of measured vs. ESPER, suggests that the discrepancy is due to regional differences relative to the average forcing employed within the ESPER model.

The main drivers of $pCO_2$ seasonality are temperature and $C_T$, with little contribution from $A_T$ or salinity (Fig. 2). Each contributes 57%, 34%, 8%, and 1% of the $pCO_2$ seasonality, respectively. The effects of temperature and $C_T$ on $pCO_2$ are out of phase, which cancels out much of their seasonal impact on $pCO_2$. In turn, $C_T$ is driven by gas exchange, net ecosystem metabolism and mixing (Wolfe, 2022)[16]. On a decadal timescale, increasing $C_T$ is the only significant driver of $pCO_2$, contributing 93% (Supplementary Fig. 3). Similarly, $C_T$ is responsible for >90% of the trends in the other carbonate variables shown in Fig. 1 and Table 1. Although it is beyond the scope of this work, a mixed layer carbon budget at station 90.90 is the subject of a separate manuscript in progress.

The measured sea surface $pCO_2$ trend matches the atmospheric $CO_2$ trend over the same timeframe, although the sea surface $pCO_2$ has significantly greater variability than atmospheric $pCO_2$, a feature common to all ocean time series (Fig. 3)[29,30]. The mean sea surface $pCO_2$ seasonal cycle derived from the CalCOFI bottle data also exhibits a greater amplitude (42 vs. 29 µatm) and a phase shifted maximum (July vs. September) compared to the climatological sea surface $pCO_2$ (Fig. 4, based on the Landschützer climatology[25] and SeaFlux product[26]). Perhaps most importantly, the measured sea surface $pCO_2$ at station 90.90 is, on average, 15 µatm higher than the products derived from the Surface Ocean $CO_2$ Atlas (SOCAT) database[23], a discrepancy large enough to lead to characterization of this location as a $CO_2$ source (when using the measured data) rather than a sink (when using e.g., the SeaFlux data products) to the atmosphere (Fig. 3).

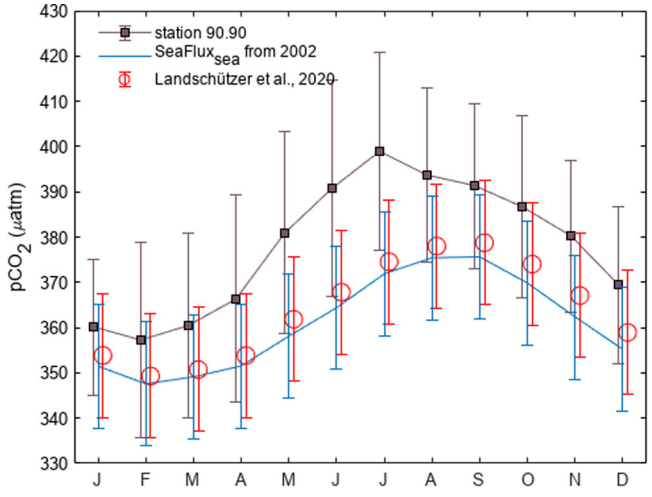


**Fig. 4 Hydrography vs. climatology.** The measured $pCO_2$ cycle at station 90.90 (computed from $A_T$ and $C_T$) compared to the Landschützer et al. (2020) climatology at station 90.90. The climatology was adjusted to a mean year of 2002 by applying our observed slope of −1.5 µatm yr$^{-1}$ (Table 1), and by the scaling of Fay et al. (2021) to generate the SeaFlux data product (sampled for year 2002). Error bars for 90.90 are identical to Fig. 1j. Error bars shown for the Landschützer climatology and SeaFlux product are 13.7 µatm, the RMSE reported in Table 2 in ref. [25].

The higher mean and more variable $pCO_2$ of the time series relative to the data products highlights the continued need for direct measurements. An important next step should be assimilating the data presented in this work into empirical algorithms and climatology products of the $CO_2$ system at the station 90.90 study site. There is little doubt that future versions of products such as ESPER and SeaFlux will benefit by incorporating new measurements such as the 90.90 data as well as assimilating new data sets (e.g., using SOCAT data in ESPER).

## Conclusions

This work establishes station 90.90 as one of very few long-standing marine inorganic carbon time series[9], with various unique properties. Over 37 years, the surface ocean at station 90.90 has decreased in pH by 0.0015 yr$^{-1}$ and increased in $pCO_2$ and $C_T$ by 1.6 µatm yr$^{-1}$ and 0.7 µmol kg$^{-1}$ yr$^{-1}$, respectively. While these trends are in line with other open ocean trends documented in the Central North Pacific, and Sargasso Sea[9], we found that widely used empirical proxy relationships[24] introduced a 40% bias in the rate of $CO_2$ local uptake, underscoring the need for sustained measurements. We also report a strong annual cycle in carbonate system variables, with dominant control of the seasonal cycle by temperature and total inorganic carbon. In contrast, the long-term secular trend in carbonate system variables is directly related to an increase in total inorganic carbon.

## Methods

**Sampling at station 90.90**. CalCOFI station 90.90 is located at 31.4°N, 122°W, approximately 450 km from shore, with a water depth of approximately 4000 m. All observations discussed here were collected near the sea surface (0–20 m), with an average depth of 5.2 m. Although a small subset of these measurements (2009–2015) have been publicly available for several years (see data availability), the remaining 22 years of observations have not been published until this work.

Observations used in this work cover the period 1984–2021 with a gap from 2002 to 2008. Bottle samples were collected on quarterly CalCOFI cruises at station 90.90. Mercuric chloride was added (as a biocide and preservative to final concentration of 50 µM) and the samples were sealed and stored in borosilicate glass bottles following best practices[31]. Storage times ranged from one month to multiple years before analysis.

**Analytical methods**. Bottle samples were analyzed for total alkalinity ($A_T$) and dissolved inorganic carbon ($C_T$). $A_T$ was measured using a closed cell titration[32] until 1992 and an open cell titration[33] after 1992. $C_T$ was measured using vacuum extraction and manometry[34,35] until 1992, coulometry[36] from 1992 to 2015 and an infrared (IR) analyzer[37,38] after 2015. Throughout the record, $C_T$ has been traceable to a Scripps manometer (either directly or via Certified Reference Materials[39] after 1992) which, in parallel with NOAA, defines the WMO mole fraction scale for $CO_2$ in air. $A_T$ has been measured using the traceable practices (acid standardization, weighing) and data processing that now define the $A_T$ of Certified Reference Materials[33]. The various methods used over the years for both $A_T$ and $C_T$ differ primarily in their precision and therefore accuracy of $A_T$ and $C_T$ is estimated to range from 2 to 5 µmol kg$^{-1}$ and 1–3 µmol kg$^{-1}$, respectively, over the dataset, reflecting the range of precisions of instruments used with the low end of the range representing the uncertainty of the reference material or method.

**Calculating additional carbonate chemistry parameters**. The partial pressure of $CO_2$ in seawater ($pCO_2$), pH (total scale), carbonate ion concentration ($[CO_3^{2-}]$), saturation states of aragonite and calcite ($\Omega_{aragonite}$, $\Omega_{calcite}$), and Revelle Factor ($\partial \ln[CO_2]/\partial \ln C_T$), were calculated in MATLAB using CO2SYS[40] from $A_T$, $C_T$, temperature and salinity with carbonic acid equilibrium coefficients reported in Lueker et al.[35] and other constants as recommended by the Guide to Best Practices[31] along with the borate-salinity relationship of Lee et al.[41]. Based on propagation of error through CO2SYS, the measurement uncertainty in $C_T$ and $A_T$ may lead to an error in $pCO_2$ in the range 6–10 µatm. The choice of input constants (or choice of uncertainty one assigns to the constants) used in CO2SYS presents a significant source of bias in derived values that would negligibly affect the reported slopes in Table 1, but significantly affect the mean $pCO_2$ and other derived parameters in Figs. 1, 3, and 4. Resolving such biases in derived vs measured $CO_2$ system parameters has long been a central focus of marine carbonate chemists[42–44] and may indeed prove to be part of the apparent ~15 µatm bias between the $pCO_2$ derived from CalCOFI bottle data and products based on underway $pCO_2$ (Figs. 3 and 4). $A_T$ and $C_T$ were salinity normalized (indicated by n$A_T$ and n$C_T$,) to the average salinity of the time series (33.3, $n = 107$).

**Seasonal cycle**. Monthly binning is a common approach used to extract the seasonal cycle[45,46]. In this work the 12-month climatology was computed from quarterly observations using a 3-month sliding bin. Where, for example, April is represented as the average of all observations from March, April, and May. Due to variability in the scheduling of CalCOFI cruises, there are some observations in each month before binning (Supplementary Fig. 2). The resulting 12-month climatology was used to seasonally detrend the observations as removing periodic signals is a best practice for assessing OA trends[47]. The climatology was used to calculate the relative contributions of salinity, temperature, $A_T$, and $C_T$ to the seasonal cycle of $pCO_2$. The climatology of a single parameter and the average of the remaining three were used with

CO2SYS to calculate individual contributions, at time t, as follows,

$$\triangle pCO_{2,t}^{\text{temperature}} = pCO_2\left(\bar{A_T}, \bar{C_T}, \bar{S}, T_t\right) - p\bar{C}O_2 \quad (1)$$

$$\triangle pCO_{2,t}^{\text{salinity}} = pCO_2\left(\bar{A_T}, \bar{C_T}, S_t, \bar{T}\right) - p\bar{C}O_2 \quad (2)$$

$$\triangle pCO_{2,t}^{C_T} = pCO_2\left(\bar{A_T}, C_{Tt}, \bar{S}, \bar{T}\right) - p\bar{C}O_2 \quad (3)$$

$$\triangle pCO_{2,t}^{A_T} = pCO_2\left(A_{Tt}, \bar{C_T}, \bar{S}, \bar{T}\right) - p\bar{C}O_2 \quad (4)$$

The same procedure was used to calculate the contribution to the long-term trends in $pCO_2$ (Supplementary Fig. 3).

**Data processing**. Model I linear regression (function fitlm in MATLAB) was performed on observations (Supplementary Fig. 4, Supplementary Table 1) and seasonally detrended data (Table 1). The slope, error, $r^2$, *p*-value and *n* values are reported. PSD analysis was performed using Lomb-Scargle periodograms with the 'plomb' function in MATLAB (Supplementary Fig. 4)[48]. Observations were also compared to empirically derived proxy estimates "ESPER_MIXED"[24,40,49] and to a climatology[25] derived from data sources (Global Ocean Data Analysis Project; GLODAP[22], The Surface Ocean $CO_2$ Atlas; SOCAT[23]) including local observations form the Eastern Pacific, independent from the CalCOFI $CO_2$ record.

## Data availability

The Station 90.90 data used in this work are publicly available through the CalCOFI data portal, https://calcofi.org/data/oceanographic-data/dic/. The atmospheric $CO_2$ data from Mauna Loa are from Dr. Ralph Keeling, Scripps Institution of Oceanography (scrippsco2.ucsd.edu/data/atmospheric_co2/primary_mlo_co2_record/, https://doi.org/10.6075/J08W3BHW) or Dr. Pieter Tans, National Oceanic and Atmospheric Administration, Global Monitoring Laboratory (gml.noaa.gov/ccgg/trends/).

Received: 26 April 2023; Accepted: 18 October 2023;
Published online: 03 November 2023

## References

1. Friedlingstein, P. et al. Global Carbon Budget 2021. *Earth Syst. Sci. Data* **14**, 1917–2005 (2022).
2. Gruber, N. et al. The oceanic sink for anthropogenic $CO_2$ from 1994 to 2007. *Science* **363**, 1193 (2019).
3. Doney, S. et al. The impacts of ocean acidification on marine ecosystems and reliant human communities. *Annu. Rev. Environ. Resour.* **45**, 83–112 (2020). *Vol 45*.
4. Fassbender, A., Orr, J. & Dickson, A. Technical note: interpreting pH changes. *Biogeosciences* **18**, 1407–1415 (2021).
5. Osborne, E., Thunell, R., Gruber, N., Feely, R. & Benitez-Nelson, C. Decadal variability in twentieth-century ocean acidification in the California current ecosystem. *Nat. Geosci.* **13**, 43 (2020).
6. Turi, G., Lachkar, Z., Gruber, N. & Nunnich, M. Climatic modulation of recent trends in ocean acidification in the California current system. *Environ. Res. Lett.* **11**, 014007 (2016).
7. Chavez, F. et al. Climate variability and change response of a coastal ocean ecosystem. *Oceanography* **30**, 128–145 (2017).
8. Hewitt, R. Historical review of the oceanographic approach to fishery research. *Calif. Coop. Ocean. Fish. Investig. Rep.* **29**, 27–41 (1988).
9. Bates, N. et al. A time-series view of changing ocean chemistry due to ocean uptake of anthropogenic $CO_2$ and ocean acidification. *Oceanography* **27**, 126–141 (2014).
10. Phillips, H. E. & Joyce, T. M. Bermuda's tale of two time series: hydrostation S and BATS*. *J. Phys. Oceanogr.* **37**, 554–571 (2007).
11. Olafsson, J., Olafsdottir, S. R., Benoit-Cattin, A. & Takahashi, T. The irminger sea and the iceland sea time series measurements of sea water carbon and nutrient chemistry 1983–2008. *Earth Syst. Sci. Data* **2**, 99–104 (2010).
12. Benway, H. M. et al. Ocean time series observations of changing marine ecosystems: an era of integration, synthesis, and societal applications. *Front. Mar. Sci.* **6**, 393 (2019).
13. Checkley, D. & Barth, J. Patterns and processes in the California current system. *Prog. Oceanogr.* **83**, 49–64 (2009).
14. Ma, D., Gregor, L. & Gruber, N. Four decades of trends and drivers of global surface ocean acidification. *Glob. Biogeochem. Cycles* **37**, e2023GB007765 (2023).
15. Rasmussen, L. et al. A century of southern california coastal ocean temperature measurements. *J. Geophys. Res. Oceans* **125**, e2019JC015673 (2020).
16. Wolfe, W. H. Observations of seawater carbonate chemistry in the Southern California current. *Scripps Institution of Oceanography* vol. Ph.D. Oceanography (University of California, San Diego, 2022).
17. Roobaert, A. et al. The spatiotemporal dynamics of the sources and sinks of $CO_2$ in the global coastal ocean. *Glob. Biogeochem. Cycles* **33**, 1693–1714 (2019).
18. Di Lorenzo, E. & Mantua, N. Multi-year persistence of the 2014/15 North Pacific marine heatwave. *Nat. Clim. Change* **6**, 1042 (2016). +.
19. Jacox, M. et al. Impacts of the 2015-2016 El Nino on the California current system: early assessment and comparison to past events. *Geophys. Res. Lett.* **43**, 7072–7080 (2016).
20. Lilly, L. E. et al. Biogeochemical anomalies at two Southern California current system moorings during the 2014–2016 warm anomaly-El Niño Sequence. *J. Geophys. Res. Oceans* **124**, 6886–6903 (2019).
21. Vance, J., Currie, K., Zeldis, J., Dillingham, P. & Law, C. An empirical MLR for estimating surface layer DIC and a comparative assessment to other gap-filling techniques for ocean carbon time series. *Biogeosciences* **19**, 241–269 (2022).
22. Olsen, A. et al. An updated version of the global interior ocean biogeochemical data product, GLODAPv2.2020. *Earth Syst. Sci. Data* **12**, 3653–3678 (2020).
23. Bakker, D. C. E. et al. A multi-decade record of high-quality $fCO_2$ data in version 3 of the Surface Ocean $CO_2$ Atlas (SOCAT). *Earth Syst. Sci. Data* **8**, 383–413 (2016).
24. Carter, B. et al. New and updated global empirical seawater property estimation routines. *Limnol. Oceanogr. Methods* **19**, 785–809 (2021).
25. Landschützer, P., Laruelle, G., Roobaert, A. & Regnier, P. A uniform $pCO_2$ climatology combining open and coastal oceans. *Earth Syst. Sci. Data* **12**, 2537–2553 (2020).
26. Fay, A. R. et al. SeaFlux: harmonization of air–sea $CO_2$ fluxes from surface $pCO_2$ data products using a standardized approach. *Earth Syst. Sci. Data* **13**, 4693–4710 (2021).
27. Juranek, L. W. et al. A novel method for determination of aragonite saturation state on the continental shelf of central Oregon using multi-parameter relationships with hydrographic data. *Geophys. Res. Lett.* **36**, L24601 (2009).
28. Alin, S. R. et al. Robust empirical relationships for estimating the carbonate system in the southern California current system and application to CalCOFI hydrographic cruise data (2005–2011). *J. Geophys. Res. Oceans* **117**, C05033 (2012).
29. Keeling, C. et al. Atmospheric CO2 and $13CO_2$ exchange with the terrestrial biosphere and oceans from 1978 to 2000: observations and carbon cycle implications. in *A history of atmospheric CO2 and its effects on plants, animals, and ecosystems* 83–113 https://doi.org/10.1007/0-387-27048-5_5 (Springer, 2005).
30. Keeling, R. & Keeling, C. Atmospheric monthly in situ $CO_2$ data-Mauna Loa observatory, Hawaii. https://doi.org/10.6075/J08W3BHW (2017).
31. Dickson, A. G., Sabine, C. L. & Christian, J. R. Guide to best practices for ocean $CO_2$ measurements. *PICES Spec. Publ.* (2007).
32. Bradshaw, A. L., Brewer, P. G., Shafer, D. K. & Williams, R. T. Measurements of total carbon dioxide and alkalinity by potentiometric titration in the GEOSECS program. *Earth Planet. Sci. Lett.* **55**, 99–115 (1981).
33. Dickson, A. G., Afghan, J. & Anderson, G. Reference materials for oceanic $CO_2$ analysis: a method for the certification of total alkalinity. *Mar. Chem.* **80**, 185–197 (2003).
34. Lueker, T. Carbonic acid dissociation constants determined as the ratio $K_1/K_2$ from the concentration of $CO_2$ in gas and seawater equilibrium. vol. PhD (University of California, San Diego, 1998).
35. Lueker, T., Dickson, A. & Keeling, C. Ocean $pCO_2$ calculated from dissolved inorganic carbon, alkalinity, and equations for $K_1$ and $K_2$: validation based on laboratory measurements of $CO_2$in gas and seawater at equilibrium. *Mar. Chem.* **70**, 105–119 (2000).
36. Johnson, K., Sieburth, J., Williams, P. & Brandstrom, L. Coulometric total carbon-dioxide analysis for marine studies - automation and calibration. *Mar. Chem.* **21**, 117–133 (1987).
37. Goyet, C. & Snover, A. K. High-accuracy measurements of total dissolved inorganic carbon in the ocean - comparison of alternate detection methods. *Mar. Chem.* **44**, 235–242 (1993).
38. O'Sullivan, D. & Millero, F. Continual measurement of the total inorganic carbon in surface seawater. *Mar. Chem.* **60**, 75–83 (1998).
39. Dickson, A. G. Reference materials for oceanic CO2 measurements. *Oceanography* **14**, 21–22 (2001).

40. van Heuven, S., Pierrot, D. & Rae, J. MATLAB Program Developed for $CO_2$System Calculations. *ORNLCDIAC−105b* **1**, Carbon Dioxide Information Analysis Center, Oak Ridge National Laboratory, U.S. Department of Energy, Oak Ridge, Tennessee (2011).
41. Lee, K. et al. The universal ratio of boron to chlorinity for the North Pacific and North Atlantic oceans. *Geochim. Cosmochim. Acta* **74**, 1801–1811 (2010).
42. Millero, F. J. et al. The internal consistency of $CO_2$ measurements in the equatorial Pacific. *Mar. Chem.* **44**, 269–280 (1993).
43. Chen, B., Cai, W.-J. & Chen, L. The marine carbonate system of the Arctic Ocean: assessment of internal consistency and sampling considerations, summer 2010. *Mar. Chem.* **176**, 174–188 (2015).
44. Fong, M. B. & Dickson, A. G. Insights from GO-SHIP hydrography data into the thermodynamic consistency of CO2 system measurements in seawater. *Mar. Chem.* **211**, 52–63 (2019).
45. Bates, N. et al. Detecting anthropogenic carbon dioxide uptake and ocean acidification in the North Atlantic Ocean. *Biogeosciences* **9**, 2509–2522 (2012).
46. Takahashi, T. et al. Climatological distributions of pH, pCO2, total CO2, alkalinity, and CaCO3 saturation in the global surface ocean, and temporal changes at selected locations. *Mar. Chem.* **164**, 95–125 (2014).
47. Sutton, A. J. et al. Advancing best practices for assessing trends of ocean acidification time series. *Front. Mar. Sci.* **9**, 1045667 (2022).
48. VanderPlas, J. Understanding the Lomb-Scargle Periodogram. *Astrophys. J. Suppl. Ser.* **236**, 16 (2018).
49. Morgan, P. P. SEAWATER: a library of MATLAB® computational routines for the properties of sea water: Version 1.2. (1994).


## Acknowledgements

Measurements have been supported by a variety of funding sources including NSF (California Current Ecosystem Long Term Ecological Research, award OCE-16-37632), and NOAA Climate Program Office. The crew and scientists on CalCOFI cruises, and the people who made these measurements over the last 37 years are too numerous to list here but this work would not have been possible without their efforts. Guy Emanuele aided in locating historical data.

## Author contributions

W.H.W. performed sample analysis, data curation, data analysis, manuscript composition, figure preparation. T.R.M. experimental design, data analysis, manuscript composition. A.G.D. sample analysis, manuscript composition. R.G. sample collection and manuscript editing. M.D.O. experimental design and manuscript editing.

## Competing interests

The authors declare no competing interests.

## Additional information

**Supplementary information** The online version contains supplementary material available at https://doi.org/10.1038/s43247-023-01065-0.

**Correspondence** and requests for materials should be addressed to Todd R. Martz.

**Peer review information** *Communications Earth & Environment* thanks Louise Delaigue, Nicolas Gruber and Kim Currie for their contribution to the peer review of this work. Primary Handling Editors: Olivier Sulpis, Clare Davis. A peer review file is available.

**Reprints and permission information** is available at http://www.nature.com/reprints

**Publisher's note** Springer Nature remains neutral with regard to jurisdictional claims in published maps and institutional affiliations.